Effects of the Number and Spatial Layout of Distributed Storage Facilities on the Structural Resilience of Urban Stormwater Networks

Xujie Zheng
College of Architecture and Civil Engineering, Beijing University of Technology, Beijing, China

Abstract: To address the lack of quantitative criteria for configuring distributed storage ponds under a fixed total storage volume, this study quantified the effects of storage pond number and spatial layout on the structural resilience of urban stormwater drainage networks. Candidate placement nodes were selected using a topological-distance-based K-Medoids method. The fixed total storage volume was then equally allocated among different numbers of storage ponds to generate schemes with varying facility numbers and placement locations. System structural resilience was evaluated using the extended Global Resilience Analysis (GRA) method, and the Spatial Dispersion Index (SDI) was introduced to characterize the spatial dispersion of storage ponds and clarify its influence on structural resilience. The results showed that increasing the number of storage ponds improved both the mean structural resilience and its lower bound. However, structural resilience did not increase continuously with storage pond number; instead, the maximum value of 0.3938 was achieved under a moderate number of storage ponds. SDI was negatively correlated with structural resilience, and high-resilience schemes depended on the prioritized placement of key nodes. These findings indicate that increasing the number of storage ponds and achieving spatially uniform dispersion are not sufficient conditions for optimizing structural resilience. The results provide a quantitative basis for determining the number of storage ponds, controlling their spatial dispersion, and identifying key placement nodes under a fixed total storage volume.

Keywords: Distributed Storage Ponds; Global Resilience Analysis (GRA); K-Medoids Clustering; Spatial Dispersion Index (SDI); Spatial Layout

1. Introduction

Increasing extreme rainfall intensity and the expansion of impervious surfaces have increased stormwater runoff loads, making urban flooding an important issue affecting urban safety and sustainable development (Miller and Hutchins, 2017; Wang et al., 2025; Zhou et al., 2019) [7,18,22]. Stormwater drainage networks are important facilities in urban drainage systems, and their service performance directly affects the effectiveness of urban surface waterlogging control (Rossman and Huber, 2016)[12]. However, due to long-term operation, limited maintenance, and other factors, existing pipe networks are prone to structural defects such as aging, damage, leakage, sedimentation, and blockage, leading to the degradation of drainage capacity and increasing the risk of urban flooding under storm conditions (Rodríguez et al., 2012; Shin et al., 2018; Yang et al., 2026)[10,15,21]. For example, Van Bijnen et al. (2012) demonstrated that in-sewer structural defects can substantially affect the frequency, spatial distribution, and volume of urban pluvial flooding[16]. Therefore, internal structural failures have become an important factor restricting the drainage performance of existing stormwater drainage networks, improving the ability of the system to maintain drainage function under structural failure disturbances (Yan et al., 2025) [20].

Because the causes of structural failures are complex and their consequences are highly uncertain (Liu et al., 2023; Rodríguez et al., 2012)[5,10], post-event responses that rely solely on failure prediction cannot support proactive pipe network management. To quantify the ability of urban drainage systems to cope with uncertain structural failure disturbances, it is necessary to introduce a resilience perspective and quantify the ability of the system to maintain service function under internal component failures. Mugume et al.(2015) were among the first to introduce structural resilience into urban drainage system research and proposed the Global Resilience Analysis (GRA) framework, shifting the research focus from probability prediction of failure events to the evaluation of system performance responses under a large number of potential failure scenarios[9]. This framework constructs random cumulative pipe failure scenarios and analyzes the response changes of system performance under different structural failure levels(Kamali et al., 2022), providing an important methodological basis for evaluating the structural resilience of stormwater drainage networks. Based on this framework, Mugume and Butler (2017) applied GRA to functional resilience assessment to analyze performance changes in urban drainage systems under different extreme rainfall scenarios[8]. On this basis, Rodriguez et al.(2023) pointed out that resilience assessment for specific threats, if focusing only on the performance outcomes after system failure, is difficult to fully reflect the variation patterns of system responses under different threat intensities [11]. Therefore, their study extended the existing GRA to threat-impact analysis under continuous long-term hydrological simulation conditions, taking the threat imposed on the system as stress and the performance response generated by the system as strain, and accordingly constructing a stress-strain curve. The area under the curve was then used to characterize the cumulative performance loss of the system within a certain threat range and served as a quantitative resilience indicator.

Structural resilience assessment can represent system performance loss under structural failure disturbances as comparable quantitative indicator, providing a tool for analyzing the effectiveness of engineering measures in improving the system’s resistance to failures (Luo et al., 2024; Mugume et al., 2015)[6,9]. Structural failures such as pipe sedimentation and blockage can reduce pipe conveyance capacity, causing flow to accumulate in upstream areas of the failed pipe sections and inducing flooding (Fontecha et al., 2020)[1]. For this process, engineering measures that can provide detention storage space and regulate the hydraulic load of the pipe network can mitigate the degradation of system drainage performance under structural failures (Goorden et al., 2024)[2]. Storage ponds are important engineering measures for achieving detention and regulation, and can reduce the hydraulic load of pipe networks through runoff storage, peak reduction, and delayed runoff concentration (Sharior et al., 2019)[14]. However, this engineering benefit is closely related to their spatial placement strategy. For example, in terms of rainfall-runoff regulation, Wang et al. (2023) optimized the siting of stormwater storage facilities using a two-stage method and proposed a rapid screening framework for distributed storage ponds, indicating that the rational placement of storage facilities can improve system responses to storm runoff[17]. Hesarkazzazi et al. (2022) further pointed out, from the perspectives of decentralized layout and redundant path reinforcement, that a moderately dispersed layout is conducive to improving system performance and reducing construction costs[3]. Therefore, the placement strategy of storage ponds is an important factor affecting their system-level benefits.

In terms of improving structural resilience, existing studies have shown that storage ponds can improve system performance under structural failure disturbances. For example, Mugume et al. (2015) analyzed the influence of the spatial configuration of storage ponds on structural resilience and showed that, under the same total storage volume, distributed storage strategies can reduce system flooding under structural failure scenarios more effectively than centralized storage strategies [9]. Xu et al. (2024) further found that, as the failure range expands, distributed storage continues to show advantages in reducing flooding volume and shortening flooding duration [19]. However, existing studies have mainly focused on the overall comparison between centralized and distributed storage strategies, and the resulting conclusions are insufficient to directly guide engineering practice. Under the constraint of a fixed total storage volume, the relationships among the number of storage ponds, their spatial placement locations, and system structural resilience remain unclear. Therefore, it is necessary to quantitatively analyze the influence of the number–location configuration of storage ponds on the structural resilience of stormwater drainage networks under a fixed total storage volume, thereby providing a basis for pipe network rehabilitation and the optimized configuration of storage ponds.

To address the above limitations, this study quantitatively analyzes the relationship between storage pond layout schemes under a distributed strategy and system structural resilience. First, a graph clustering algorithm was introduced to screen representative candidate nodes that uniformly cover different topological locations across the entire network. On this basis, schemes with different combinations of storage pond numbers and spatial locations were constructed. A large number of structural failure scenarios were then generated for each scheme, and system structural resilience was evaluated using the extended GRA method. Meanwhile, the Spatial Dispersion Index (SDI) and key node analysis were introduced to reveal the mechanisms by which the configuration of storage ponds affects structural resilience. The results can provide a quantitative basis for the optimized configuration of distributed storage ponds in stormwater drainage network rehabilitation.

2. Methods

2.1 Study Area and Hydrodynamic Model

This study selected a stormwater drainage network in Beijing as the study object to analyze the effects of the number and spatial layout of storage ponds on system structural resilience under a fixed total storage volume. The study area has a catchment area of 3.475 hm^2, and the pipe network has a total length of approximately 0.33 km. It consists of 38 nodes, 39 pipe sections, and 38 subcatchments, as shown in Figure 1. Based on measured municipal pipe network data, a hydrodynamic model of the study area was constructed using SWMM. The model inputs included the actual pipe network topology, pipe cross-sectional dimensions, node locations, elevations, and other parameters, and the Manning coefficient of the pipes was set with reference to relevant drainage design standards (Rossman and Simon, 2022)[13]. The subcatchments were delineated using the Thiessen polygon method in ArcGIS according to the spatial distribution of stormwater manholes. The slope, imperviousness, and Horton infiltration parameters of each subcatchment were determined based on DEM, land use data, and relevant design standards. The model was finally calibrated and validated using measured waterlogging records and historical rainfall events to ensure the reliability of the simulation results.

2.2 Structural Resilience Assessment Framework

This study used the extended Global Resilience Analysis (GRA) method to evaluate the structural resilience of stormwater drainage networks under different storage pond configuration schemes. This method constructs system failure scenarios under different structural failure levels and analyzes the response process of system performance to failure disturbances, thereby characterizing the ability of the system to maintain function under internal failure conditions. In the SWMM model, structural failure scenarios were represented by the sedimentation parameters of the target pipe sections. For pipe sections selected as being in a failed state, their sedimentation depth was set equal to the pipe diameter to equivalently represent the failed state after the pipe section was removed from the pipe network.

In the structural resilience assessment, the structural failure level was represented by the proportion of failed pipe sections, and system performance P was determined by the system flooding ratio:

$$R=1-\frac{V^{flood}}{V^{in}} \quad (1)$$

Where V^{flood} is the total system flooding volume under the corresponding structural failure scenario, and V^{in} is the total system inflow volume.

(1) Construct random failure sequences (RFSs). For a stormwater drainage network containing N pipe sections, each RFS starts with a single-pipe failure as the initial scenario. Other pipes are then progressively failed based on the existing failed pipe sections, generating a sequence of structural failure scenarios with 1 to N failed pipe sections.

(2) Determine the minimum number of random failure sequences. Step (1) is repeated to generate different groups of RFSs, and the mean system performance under each structural failure level is calculated. The convergence of the sampling results is tested by comparing the deviation in mean performance between two adjacent rounds of RFS samples. When the deviation is lower than the predefined threshold, the RFS sample size is considered to meet the convergence requirement and can represent the system performance response under different structural failure levels.

(3) Construct the stress–strain curve and calculate structural resilience. Based on the converged RFS samples, the stress–strain curve is constructed by taking the structural failure level as the system stress and the mean system performance as the system strain. The area under the curve is calculated using the trapezoidal integration method and used as the structural resilience indicator to compare the structural resilience performance of stormwater drainage networks under different storage pond configuration schemes.

2.3 Candidate Node Selection Using K-Medoids

When analyzing the effects of different combinations of storage pond numbers and spatial locations on structural resilience, all possible node combinations in the pipe network need to be enumerated. Taking the case network used in this study as an example, the system contains 34 feasible placement nodes. Exhaustive enumeration of all non-empty node combinations would generate $2^{34}-1$ schemes. In addition, each scheme needs to be evaluated through a large number of structural failure scenario simulations within the GRA framework, resulting in a high computational burden. Therefore, candidate placement nodes with topological representativeness should be screened to reduce the combinatorial search space. These candidate nodes should be relatively evenly distributed in the topological space of the pipe network and cover different topological positions from upstream branches to downstream trunks, thereby providing a basis for subsequent analysis of the effects of storage pond locations on system structural resilience.

To meet these screening requirements, the K-Medoids algorithm was introduced to identify candidate nodes. Because K-Medoids selects cluster centers from actual samples in the original dataset, the identified centers are all manhole nodes, satisfying the requirement that storage ponds are placed at pipe network nodes. It should be noted that conventional clustering methods generally use Euclidean distance as the similarity metric. However, the objective of candidate node screening in this study is not to achieve uniform distribution in planar space, but to ensure adequate dispersion within the drainage network topology formed by manholes and pipes. Therefore, the shortest topological distance between nodes along pipe paths was used as the clustering distance.

Specifically, the stormwater drainage network was represented as an undirected weighted graph $G=(V,E)$, where the node set V denotes manholes, the edge set E denotes pipes, and the edge weights correspond to the actual pipe lengths. The Dijkstra algorithm was used to calculate the shortest topological distance between each pair of nodes, from which the distance matrix $d(v_i,v_j)$ was constructed. The number of candidate nodes was then set to 7, and the K-Medoids algorithm was applied to identify representative placement nodes. This setting ensures that the selected nodes remain topologically representative within the pipe network, thereby providing a basis for subsequent analysis of the effects of different placement locations on system structural resilience.

The algorithm aims to minimize the total shortest topological distance J from each node to its assigned center node:

$$J=\sum_{k=1}^{K}\sum_{v_i\in C_k} d(v_i,m_k) \quad (2)$$

where J is the total clustering cost, C_k is the k-th cluster, m_k is the center node, and $d(v_i,m_k)$ is the shortest topological distance from node v_i to m_k. Taking the minimization of J as the optimization objective can improve the ability of the selected center nodes to represent the topological spatial structure of the pipe network. Because the center nodes of K-Medoids are selected from the original node set, the resulting center nodes can be directly used as candidate placement nodes for storage ponds. The locations of the candidate nodes are shown in the following figure:

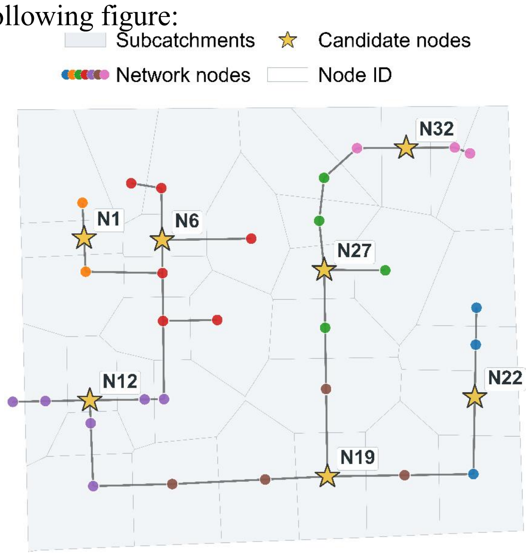

Figure 1. Spatial Distribution of Subcatchments, Drainage Network, and Candidate Storage-pond Nodes in the Study Area

2.4 Construction and Characterization of Storage Layout Scenarios

After the candidate placement nodes were determined, an ensemble of storage pond placement schemes was constructed under a fixed total storage volume. The number of storage ponds was set to n=1,2,…,7 , and all combinations of n candidate nodes were enumerated for each value of n as the corresponding placement schemes. The total storage volume V_T was kept constant across all schemes and equally allocated among the storage ponds, giving a single-pond volume of V_T/n . This generated a scheme ensemble covering different combinations of storage pond numbers and spatial locations, which provided the scenario basis for subsequent structural resilience assessment.

Existing studies have suggested that, under the same total storage volume, distributed storage layouts are more conducive to improving system structural resilience than centralized layouts. However, these studies have mainly compared centralized and distributed layouts qualitatively, without quantitatively characterizing the relationship between the degree of spatial dispersion of distributed storage ponds in the topological space of the pipe network and the improvement in structural resilience. Therefore, this study introduced the Spatial Dispersion Index (SDI) to characterize the dispersion degree of nodes in the stormwater network, as shown below:

$$SDI=\frac{2}{n(n-1)}\sum_{i=1}^{n-1}\sum_{j=i+1}^{n}d(v_i,v_j) \qquad (3)$$

where n is the number of storage ponds; v_i and v_j are the pipe network nodes where the i-th and j-th storage ponds are placed, respectively; and $d(v_i,v_j)$ denotes the shortest topological distance between nodes v_i and v_j, i.e., the number of intervening pipe sections. When n=1 , the placement scheme contains only one storage node, and pairwise topological distance is therefore not defined. This case was therefore excluded from the SDI calculation.

3. Results and Discussion

To quantify how the number and spatial locations of storage ponds affect the improvement in system structural resilience under a fixed total storage volume, the analysis focuses on three aspects: storage pond number, spatial dispersion, and key placement locations.

3.1 Effect of the Number of Storage Facilities

Figure 2 shows the distribution of system structural resilience corresponding to different numbers of storage ponds under a fixed total storage volume. The results show that increasing the number of storage ponds improved the mean level of system structural resilience, with the mean value increasing from approximately 0.19 for a single storage pond to approximately 0.35 for seven storage ponds. This result is consistent with previous studies on distributed storage, indicating that, under a fixed total storage volume, distributed placement can generally improve the average performance of system structural resilience (Mugume et al., 2015; Xu et al., 2024)[9,19]. The underlying mechanism is that distributed storage ponds can intercept runoff from different upstream areas before it enters the main pipes, thereby reducing peak flow and the hydraulic load of downstream pipe sections and decreasing the likelihood of widespread node flooding under structural failure scenarios.

However, although increasing the number of storage ponds improved the mean structural resilience, the resilience of different schemes under each pond-number level did not increase synchronously. Changes in the mean values indicate that the improvement in structural resilience gradually decreased as more storage ponds were added. The maximum values further show that the maximum structural resilience increased from approximately 0.27 to approximately 0.39 when the number of storage ponds increased from 1 to 4, reaching its peak; when the number of storage ponds continued to increase, this indicator declined. This result indicates that, under the constraint of a fixed total storage volume, there is a relatively appropriate number of storage ponds, rather than a monotonic improvement with increasing pond number. This is mainly because, under equal allocation of the total storage volume, increasing the number of storage ponds reduces the effective capacity of each individual pond. When newly added placement nodes contribute only limited flooding reduction, further dispersion of the total storage volume instead reduces the storage capacity at high-efficiency locations, thereby leading to a decline in optimal structural resilience.

In addition, the distribution characteristics of structural resilience at different pond-number levels show that, as the number of storage ponds increased, the minimum structural resilience in each group increased markedly, while the dispersion among different placement schemes gradually decreased. This phenomenon indicates that increasing the number of storage ponds not only raises the lower bound of system structural resilience, but also reduces performance differences among different spatial layout schemes. This can reduce the performance risk caused by inappropriate placement selection in engineering practice and enhance the robustness of storage pond configuration decisions.

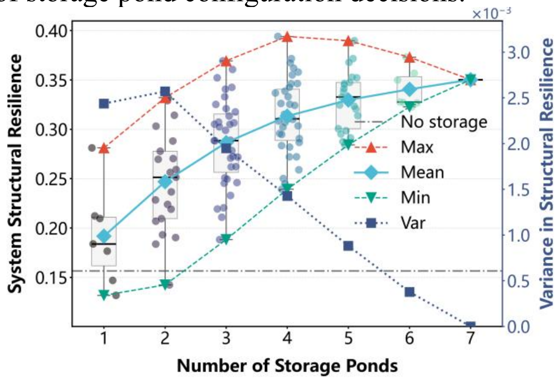

Figure 2. Evolution and Distribution of System Structural Resilience Across Varying Numbers of Detention Tanks

3.2 Effect of Spatial Dispersion on Structural Resilience

To analyze the relationship between the spatial dispersion of storage ponds and structural resilience, this study discusses different placement schemes using the Spatial Dispersion Index (SDI). Figure 3 shows the distribution relationship between SDI and system structural resilience under different numbers of storage ponds. The results show that SDI was negatively correlated with structural resilience at all pond-number levels, with correlation coefficients r ranging from -0.40 to -0.46. When all schemes were pooled, a consistent negative correlation remained, with a correlation coefficient of -0.33. This indicates that, under a fixed and equally allocated total storage volume, increasing the spatial dispersion of storage ponds did not promote structural resilience improvement. A higher SDI may indicate that part of the storage capacity was allocated to locations with lower flooding control capacity, making it difficult to effectively reduce upstream inflow from important concentration areas and thereby weakening its effect on alleviating downstream pipe loads and node flooding risks.

The distribution of the optimal schemes in each pond-number group further confirms this pattern. The optimal structural resilience schemes marked by red stars in Figure 3 were all concentrated in the low-SDI region. For n=2 and n=4, the SDI values of the optimal schemes were 3.0 and 5.5, respectively, both close to the lower-bound region of the corresponding groups. This indicates that distributed storage is not equivalent to spatially uniform dispersion; under a fixed total storage volume, moderately concentrated placement is more conducive to improving structural resilience.

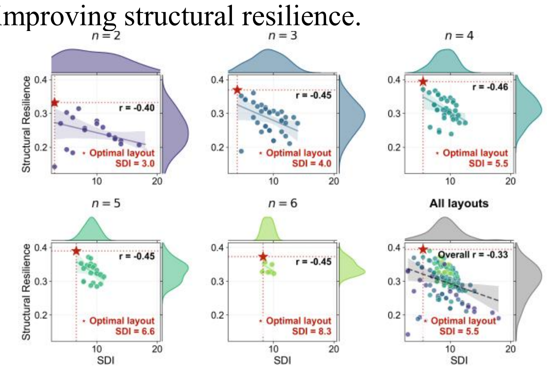

Figure 3. Relationship between the Degree of Spatial Decentralization of Detention Tanks and System Structural Resilience

In addition, as the number of storage ponds increased, the SDI range gradually narrowed, and the lower boundary shifted overall toward higher dispersion. This indicates that, within the feasible placement space, increasing the number of storage ponds makes it more difficult for placement schemes to maintain a low degree of spatial dispersion. Combined with the negative correlation between SDI and structural resilience, this spatial dispersion caused by increasing pond number does not necessarily lead to further improvement in structural resilience, but may instead limit the resilience improvement of schemes with 5, 6, and 7 storage ponds. Furthermore, the optimal schemes in each group in Figure 3 were located in the low-value region at the edge of the SDI distribution, rather than in the dense region of the SDI distribution. This indicates that the optimal placement for structural resilience is not dominated by general spatial dispersion characteristics, but depends more on the combinational relationships among specific key locations. In other words, among all feasible placement schemes in the pipe network, most location combinations have SDI values concentrated in the main distribution region, and their corresponding structural resilience is mostly at average or relatively low levels. In contrast, only a small proportion of placement combinations can substantially improve structural resilience. Therefore, maximizing structural resilience cannot rely only on increasing the number of storage ponds or increasing spatial dispersion. Instead, targeted siting and combinational optimization of storage ponds should be conducted based on the identification of key nodes.

3.3 Identification of Key Placement Nodes and Analysis of Their Underlying Mechanisms

Figure 4 shows the selection distribution of candidate nodes in different storage pond placement schemes, with the schemes ranked in descending order according to their structural resilience values. The results show that nodes 22, 27, 19, and 32 were selected more frequently in schemes with higher structural resilience, whereas nodes 12, 6, and 1 were mainly distributed in the low-resilience scheme range. This result indicates that different candidate nodes contributed differently to the improvement of structural resilience, and that system resilience enhancement depended on a small number of key placement nodes. Regardless of the number of storage ponds, prioritizing these core nodes was a prerequisite for achieving optimal structural resilience. In contrast, the remaining nodes, namely nodes 1, 6, and 12, had relatively limited effects on resilience improvement and mainly played an auxiliary role.

Figure 5 shows the storage pond locations of the optimal schemes under different pond-number groups. When the number of storage ponds increased from 1 to 4, the storage ponds in the optimal schemes were sequentially placed at nodes 19, 22, 27, and 32 in the right-side branch area of the pipe network. During this stage, the optimal structural resilience of the system increased steadily with the number of storage ponds and reached the maximum value of 0.3938 when four storage ponds were placed. Combined with Figure 4, these nodes were all frequently selected in high-structural-resilience schemes, indicating that these locations made strong contributions to system resilience improvement. When the number of storage ponds was further increased, the newly added ponds were gradually placed at low-frequency selected nodes, and the optimal structural resilience of the system instead declined. This result indicates that, after the key nodes had been largely selected, further increasing the number of storage ponds shifted the additional storage capacity toward non-key locations. Because these nodes contributed relatively little to runoff reduction and downstream hydraulic load alleviation, while also dispersing the storage capacity that could otherwise be allocated to key nodes, they could hardly further improve the optimal structural resilience of the system. Therefore, the optimal layout for system structural resilience does not depend on continuously increasing the number of storage ponds or blindly dispersing them in space, but rather on the accurate identification of key nodes and the prioritized allocation of storage capacity.

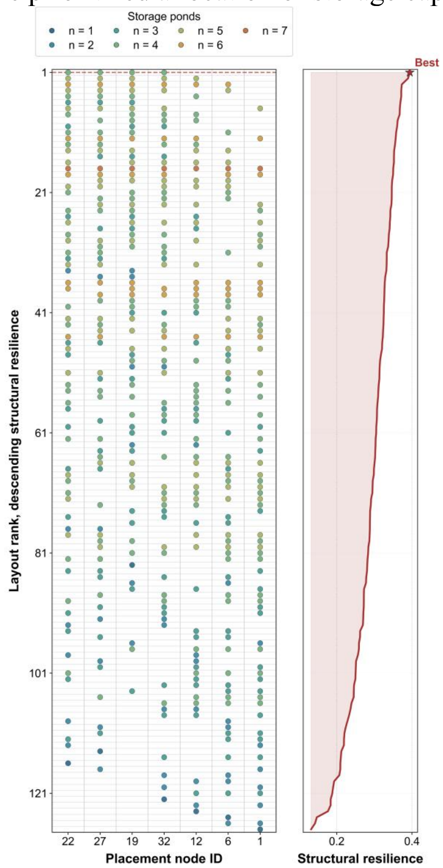

Figure 3. Distribution of All Siting Schemes and Selected Node Locations for Detention Tanks

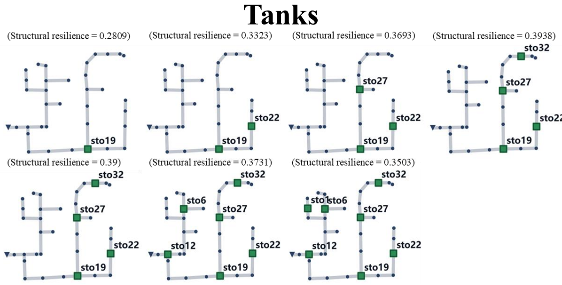

Figure 4. Optimal Storage-pond Layouts and Corresponding Structural Resilience under Different Numbers of Storage ponds

4. Conclusions

This chapter quantified system structural resilience using the extended Global Resilience Analysis (GRA) method. Under a fixed total storage volume, the total capacity was equally allocated among different numbers of storage ponds to quantitatively analyze how storage pond number and spatial location affect the ability of the system to resist structural failures. The main conclusions are as follows:

(1) A K-Medoids-based candidate node screening method using topological distance was constructed. This method used topological distance, which reflects the actual connectivity of the pipe network, as the distance metric. It enabled the candidate nodes to be relatively evenly distributed in the topological space of the drainage network, thereby providing a scheme basis for subsequent analysis of the effects of different spatial locations on system structural resilience.

(2) The effect of storage pond number on structural resilience was analyzed when the fixed total storage volume was equally allocated among different numbers of storage ponds. The results show that increasing the number of storage ponds improved both the mean level and lower bound of system structural resilience and reduced the risk of low efficiency caused by inappropriate placement selection, thereby enhancing the robustness of storage pond schemes. Under a fixed total storage volume, the optimal structural resilience reached the maximum value of 0.3938 when four storage ponds were placed. Thereafter, as the number of storage ponds continued to increase, the optimal structural resilience declined, indicating that simply increasing the number of storage ponds cannot continuously improve the upper limit of system performance.

(3) The relationship between spatial dispersion and structural resilience was revealed. SDI showed a clear negative correlation with structural resilience, indicating that, under equal allocation of the total storage capacity, a more dispersed layout of storage ponds does not necessarily lead to greater improvement in structural resilience. Compared with highly uniformly dispersed layouts, moderately concentrated placement schemes are more conducive to the effective use of limited storage capacity. As the number of storage ponds increases, it becomes more difficult for the schemes to maintain a low dispersion degree. This passive dispersion caused by the increase in storage pond number limits the potential improvement in optimal structural resilience and is an important reason for the decline in optimal resilience when more storage ponds are placed.

(4) The dominant role of key placement nodes in the optimal improvement of structural resilience was revealed. Nodes 19, 22, 27, and 32 showed high selection frequencies in schemes with higher structural resilience and appeared sequentially in the optimal schemes as the number of storage ponds increased from 1 to 4, indicating that they are important placement nodes for improving structural resilience. After these nodes were selected, newly added storage ponds gradually shifted to nodes with low selection frequencies. Because these nodes have relatively limited effects on alleviating downstream loads, the potential improvement in optimal structural resilience was constrained. Therefore, under a fixed total storage volume, structural resilience optimization should shift from increasing the number of storage ponds and promoting spatially uniform dispersion to identifying and prioritizing key placement nodes.

References

[1] Fontecha, J.E., Guaje, O.O., Duque, D., Akhavan-Tabatabaei, R., Rodríguez, J.P., Medaglia, A.L., 2020. Combined maintenance and routing optimization for large-scale sewage cleaning. Ann. Oper. Res. 286, 441–474. https://doi.org/10.1007/s10479-019-03342-8

[2] Goorden, M.A., Larsen, K.G., Nielsen, J.E., Nielsen, T.D., Qian, W., Rasmussen, M.R., Srba, J., Zhao, G., 2024. Optimal control strategies for stormwater detention ponds. Nonlinear Anal. Hybrid Syst 53, 101504. https://doi.org/10.1016/j.nahs.2024.101504

[3] Hesarkazzazi, S., Bakhshipour, A.E., Hajibabaei, M., Dittmer, U., Haghighi, A., Sitzenfrei, R., 2022. Battle of centralized and decentralized urban stormwater networks: from redundancy perspective. Water Res. 222, 118910. https://doi.org/10.1016/j.watres.2022.118910

[4] Kamali, B., Ziaei, A.N., Beheshti, A., Farmani, R., 2022. An open-source toolbox for investigating functional resilience in sewer networks based on global resilience analysis. Reliab. Eng. Syst. Saf. 218, 108201.

https://doi.org/10.1016/j.ress.2021.108201

[5] Liu, W., He, Y., Liu, Z., Luo, H., Liu, T., 2023. A bilevel data-driven method for sewer deposit prediction under uncertainty. Water Res. 231, 119588. https://doi.org/10.1016/j.watres.2023.119588

[6] Luo, X., Liu, P., Cheng, Q., Liu, W., Zhou, C., Zheng, Y., Wang, D., Cheng, L., 2024. Reinforcing resilience for integrated design of green and grey infrastructure with real-time control rules by considering system failures. J. Hydrol. 638, 131498. https://doi.org/10.1016/j.jhydrol.2024.131498

[7] Miller, J.D., Hutchins, M., 2017. The impacts of urbanisation and climate change on urban flooding and urban water quality: a review of the evidence concerning the United Kingdom. J. Hydrol.: Reg. Stud. 12, 345–362. https://doi.org/10.1016/j.ejrh.2017.06.006

[8] Mugume, S.N., Butler, D., 2017. Evaluation of functional resilience in urban drainage and flood management systems using a global analysis approach. Urban Water J. 14, 727–736. https://doi.org/10.1080/1573062X.2016.1253754

[9] Mugume, S.N., Gomez, D.E., Fu, G., Farmani, R., Butler, D., 2015. A global analysis approach for investigating structural resilience in urban drainage systems. Water Res. 81, 15–26. https://doi.org/10.1016/j.watres.2015.05.030

[10] Rodríguez, J.P., McIntyre, N., Díaz-Granados, M., Maksimović, Č., 2012. A database and model to support proactive management of sediment-related sewer blockages. Water Res. 46, 4571–4586. https://doi.org/10.1016/j.watres.2012.06.037

[11] Rodríguez, M., Fu, G., Butler, D., Yuan, Z., Cook, L., 2023. Global resilience analysis of combined sewer systems under continuous hydrologic simulation. J. Environ. Manage. 344, 118607. https://doi.org/10.1016/j.jenvman.2023.118607

[12] Rossman, Lewis A.; Huber, Wayne C., 2016. Storm Water Management Model Reference Manual Volume I – Hydrology (Reference Manual No. EPA/600/R-14/334). U.S. Environmental Protection Agency, Washington, DC.

[13] Rossman, Lewis A., Simon, Michelle A., 2022. Storm Water Management Model User's Manual Version 5.2 (User's Manual). U.S. Environmental Protection Agency.

[14] Sharior, S., McDonald, W., Parolari, A.J., 2019. Improved reliability of stormwater detention basin performance through water quality data-informed real-time control. J. Hydrol. 573, 422–431. https://doi.org/10.1016/j.jhydrol.2019.03.012

[15] Shin, S., Lee, G., Ahmed, U., Lee, Y., Na, J., Han, C., 2018. Risk-based underground pipeline safety management considering corrosion effect. J. Hazard. Mater. 342, 279–289. https://doi.org/10.1016/j.jhazmat.2017.08.029

[16] Van Bijnen, M., Korving, H., Clemens, F., 2012. Impact of sewer condition on urban flooding: an uncertainty analysis based on field observations and monte carlo simulations on full hydrodynamic models. Water Sci. Technol. 65, 2219–2227. https://doi.org/10.2166/wst.2012.134

[17] Wang, M., Li, M., Sweetapple, C., 2023. A new framework for distributed storage tanks placement based on a resilience characteristic metric and reduced modelling. J. Environ. Manage. 342, 118098. https://doi.org/10.1016/j.jenvman.2023.118098

[18] Wang, Y., Zhang, Q., Zhang, J., Lin, K., 2025. Impact of 2D and 3D factors on urban flooding: spatial characteristics and interpretable analysis of drivers. Water Res. 280, 123537. https://doi.org/10.1016/j.watres.2025.123537

[19] Xu, K., Zhang, X., Bin, L., Shen, R., 2024. An improved global resilience assessment method for urban drainage systems: a case study of haidian island, south China. J. Environ. Manage. 360, 121135. https://doi.org/10.1016/j.jenvman.2024.121135

[20] Yan, H., Yang, Q., Wang, S., Tian, W., He, Z., Wang, J., Fu, G., Xia, S., Xin, K., Tao, T., 2025. Enhancement of urban drainage system resilience by artificial intelligence: a comprehensive review. ACS ES&T Eng. 5, 2701–2728. https://doi.org/10.1021/acsestengg.5c00700

[21] Yang, J., Zayed, T., Arimiyaw, D., Nashat, M., Liu, X., Ibrahim, A., 2026. Structural

failure in urban sewer pipelines: a comprehensive review from analysis to intervention techniques. Tunnelling Underground Space Technol. 167, 107027. https://doi.org/10.1016/j.tust.2025.107027

[22] Zhou, Q., Leng, G., Su, J., Ren, Y., 2019. Comparison of urbanization and climate change impacts on urban flood volumes: importance of urban planning and drainage adaptation. Sci. Total Environ. 658, 24–33. https://doi.org/10.1016/j.scitotenv.2018.12.184